

1 Discovery of a broadly-neutralizing human antibody that can rescue
2 mice challenged with neurotoxin-rich snake venoms

3 Line Ledsgaard¹, Jack Wade¹, Kim Boddum², Irina Oganesyan³, Julian Harrison³, Timothy P. Jenkins¹,
4 Pedro Villar⁴, Rachael A. Leah⁴, Renato Zenobi³, John McCafferty⁴, Bruno Lomonte⁵, José M.
5 Gutiérrez^{5*}, Andreas H. Laustsen^{1*}, Aneesh Karatt-Vellatt^{4*}

6 ¹Department of Biotechnology and Biotherapeutics, Technical University of Denmark; DK-2800 Kongens Lyngby,
7 Denmark

8 ²Sophion Bioscience, DK-2750 Ballerup, Denmark

9 ³Laboratory of Organic Chemistry, Department of Chemistry and Applied Biosciences, ETH Zurich, CH-8093
10 Zurich, Switzerland

11 ⁴IONTAS Ltd.; Cambridgeshire CB22 3FT, United Kingdom

12 ⁵Instituto Clodomiro Picado, Facultad de Microbiología, Universidad de Costa Rica; San José 11501-2060, Costa
13 Rica

14 *Correspondence: jose.gutierrez@ucr.ac.cr (J.M.G); ahola@bio.dtu.dk (A.H.L.); akv@maxion.co.uk (A.K-V.)

15 **Abstract:**

16 Snakebite envenoming continues to claim many lives across the globe, necessitating the
17 development of improved therapies. To this end, human monoclonal antibodies may possess
18 advantages over current plasma-derived antivenoms by offering superior safety and improved
19 neutralization capacity. However, as new antivenom products may need to be polyvalent, *i.e.*,
20 target multiple different snake species, without dramatically increasing dose or cost of
21 manufacture, such monoclonal antibodies need to be broadly-neutralizing. Here, we report the
22 establishment of a pipeline for the discovery of high affinity broadly-neutralizing human
23 monoclonal antibodies. We further demonstrate its utility by discovering an antibody that can
24 prevent lethality induced by *N. kaouthia* whole venom at an unprecedented low molar ratio of one
25 antibody per toxin, and which also prolongs survival of mice injected with *Dendroaspis polylepis*
26 or *Ophiophagus hannah* whole venoms.

28 INTRODUCTION

29 Each year, snakebite envenoming exacts a high death toll and leaves hundreds of thousands of
30 other victims maimed for life¹. Antivenoms based on polyclonal antibodies isolated from the
31 plasma of immunized animals are currently the only specific treatment option against severe
32 envenomings^{2,3}. While these medicines are essential and life-saving, and will remain a cornerstone
33 in snakebite therapy for years to come, an opportunity now exists to modernize treatment by
34 exploiting the benefits of recombinant DNA and antibody technology⁴. Indeed, recombinant
35 antibodies have already been generated against a variety of snake venom toxins^{5–8}. Moreover,
36 within this area of research, it has been demonstrated that monoclonal antibodies targeting snake
37 venom toxins can be developed using various platforms, such as phage display technology⁶, an *in*
38 *vitro* methodology that can be used to actively select for antibodies with high-affinity and cross-
39 reactivity^{7,8}. In addition, the use of human antibody libraries in combination with phage display
40 technology allows for the discovery of fully human antibodies, that are likely to have high
41 treatment tolerability in patients.

42 It has been speculated that monoclonal antibodies developed by these means could be used
43 to formulate recombinant antivenoms that elicit fewer adverse reactions, are cost-competitive to
44 existing therapy, and can be fine-tuned to have superior efficacy^{9–13}. Phage display technology
45 could be particularly valuable for discovering monoclonal antibodies against highly potent toxins
46 with low immunogenicity that fail to elicit a strong antibody response in animals used for
47 immunization^{14,15}. This is the case for low molecular mass neurotoxins and cytotoxins of the three-
48 finger toxin (3FTx) family, which are abundant in Elapidae venoms, such as cobra and mamba
49 venoms^{16–19}. However, antibodies derived directly from naïve libraries often lack sufficiently high
50 affinity to enable toxin neutralization⁸. Affinity can be improved by further site-directed or random

51 mutagenesis of the antibody paratopes, which can also lead to broadening of the neutralizing
52 capacity of naïve antibodies²⁰. However, besides mutation of the antibody binding regions,
53 retaining the heavy chains and exploring alternative light chains, a technique known as light chain-
54 shuffling, has shown significant promise as well^{14,21}. Here, a phage display library is generated by
55 paring a heavy or light chain from a specific antibody with a naïve repertoire of the partner chain
56 and performing a new selection campaign⁸. Nevertheless, until now it remained unknown whether
57 this technology could be used to generate antibodies that possess high affinity while
58 simultaneously having a broad neutralization capacity, *i.e.*, are able to neutralize several related
59 toxins from the venoms of different snake species.

60 Previously, using a naïve human scFv-based phage display library⁸, we described the
61 discovery and characterization of the human monoclonal antibody, 368_01_C05, against α -
62 cobra toxin (P01391), a potent neurotoxin from the monocled cobra, *Naja kaouthia*. Notably, this
63 antibody could prolong the survival of mice injected with lethal doses of α -cobra toxin, although it
64 failed to prevent lethality⁸. As a follow-up development, in the present study we constructed light-
65 chain-shuffled antibody libraries based on this clone with the aim of using a phage display-based
66 cross-panning campaign to simultaneously improve the affinity and expand the neutralizing
67 capacity of the antibody against α -neurotoxins from the venoms of several snake species. Cross-
68 panning was carried out between α -cobra toxin²² and α -elapitoxin²³, a neurotoxin from the venom
69 of the black mamba, *Dendroaspis polylepis*¹⁸. These two α -neurotoxins share 70% sequence
70 identity and both cause neuromuscular blockade by binding to the nicotinic acetylcholine receptor
71 (nAChR) in muscle cells.

72 In this work, we “cross-panned” the chain-shuffled scFv library on these two toxins under
73 stringent conditions to discover antibodies with improved affinity and cross-reactivity in

74 comparison to the parent antibody. Using this strategy, we were able to generate an antibody which
75 not only has improved affinity to α -cobratoxin, but also significantly broadened cross-
76 neutralization capacity against other α -neurotoxins from the venoms of elapid snakes from the
77 genera *Dendroaspis*, *Ophiophagus*, *Bungarus*, and *Naja*.

78 **RESULTS**

79 **Affinity maturation, cross-panning selections, and scFv characterization**

80 Human light-chain-shuffled scFv-based phage display libraries were created by paring the heavy
81 chain of antibody 368_01_C05 with a naïve repertoire of human light chains. Then, phage display
82 cross-panning selections using two toxins with 70% sequence identity, α -cobratoxin from *N.*
83 *kaouthia* and α -elapitoxin from *D. polylepis*, were conducted according to the overview provided
84 in Fig. 1A. Phage display selection outputs from the third round were subcloned into the
85 pSANG10-3F expression vector, and 736 monoclonal scFvs were tested for their ability to bind to
86 α -cobratoxin, α -elapitoxin, and streptavidin in both direct dissociation-enhanced lanthanide
87 fluorescence immunoassays (DELFIA) and expression-normalized capture (ENC) DELFIA. From here, 203 scFvs (all displaying binding to at least one of the two toxins with negligible
88 binding to streptavidin) were randomly selected for sequencing. Out of these, 67 scFvs were
89 unique according to the sequence of their light chain CDR3 region, 2 of them having kappa light
90 chains and the remaining 65 having lambda light chains. The top 62 clones, based on sequence
91 diversity and binding behavior, were reformatted to the fully human IgG1 format. Following
92 expression in HEK293 cells, ENC DELFIA were run using the crude expression supernatant to
93 rank the IgG binding to α -cobratoxin, α -elapitoxin, a venom fraction from *N. melanoleuca* (Nm8)
94 containing a long neurotoxin homologous to OH-55 (Q53B58) and long neurotoxin 2 (P01388)²⁴,
95 as well as streptavidin. This revealed that more than half of the clones were cross-reactive against

97 all three toxins/venom fractions, demonstrating significant improvement in both binding and cross-
98 reactivity when compared to the parental antibody.

99 To help guide the selection of lead candidates, the suitability of the 62 clones for future antibody
100 development was investigated by characterizing biophysical properties that are indicative of their
101 “developability” profiles. To this purpose, we analyzed the purity and non-specific column
102 interaction pattern of all IgGs using size-exclusion chromatography (SEC). In addition an AC-
103 SINS assay²⁵ was employed to asses propensity for self-aggregation. For this analysis, we also
104 included an IgG from a previous study (2552_02_B02)⁸, that had been reported to neutralize
105 lethality induced by *N. kaouthia* whole venom *in vivo*, but had never been characterized for cross-
106 reactivity to other long chain α -neurotoxins nor been analyzed for its “developability” properties.

107 The SEC data (% monomeric content and relative elution volumes - a metric for assessing non-
108 specific interaction with the SEC column), AC-SINS shifts, binding data, expression yields (full
109 dataset see Table S1), as well as light chain germ-line diversity were used to select the top six
110 antibody candidates for further characterization. These antibodies were named as follows:
111 2551_01_A12, 2551_01_B11, 2554_01_D11, 2555_01_A01, 2555_01_A04, and 2558_02_G09
112 (Fig. 1B and Table 1). Additionally, the data showed that the previously published IgG
113 2552_02_B02 had an extremely poor developability score, both judged by its late elution in the
114 SEC analysis and its high shift in the AC-SINS assay. In fact, this antibody performed at a similarly
115 poor level as the ‘poor developability’ control (bococizumab, AC-SINC shift of 33 nm) that was
116 used for comparison, whereas all antibodies derived from the 368_01_C05 parental clone
117 possessed developability profiles similar to the ‘good developability’ control antibody
118 (Aliricumab, AC-SINS shift of 3 nm). In addition, 2552_02_B02 showed no cross-reactivity to

119 any of the long chain α -neurotoxins it was tested against, clearly distinguishing its binding profile
120 from the antibodies derived from the 368_01_C05 parent (Fig. 1B).

121 **Table 1. AC-SINS shift, SEC analysis results (% monomer content and relative elution**
122 **volume), and transient expression yields** for the top six chain-shuffled IgGs (2551_01_A12,
123 2551_01_B11, 2554_01_D11, 2555_01_A01, 2555_01_A05, and 2558_02_G09) in comparison
124 with the parental IgG (368_01_C05). IgG 2552_02_B02 from a previous study was also included.

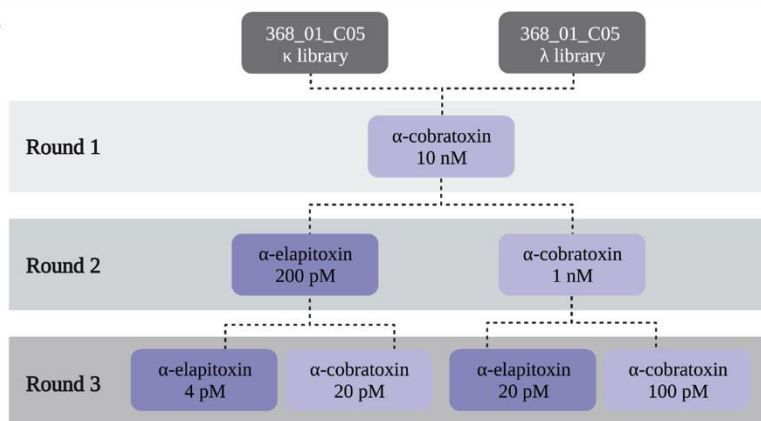
Antibody ID	AC-SINS	SEC analysis		Production
	Shift (nm)	Monomer (%)	Elution (mL)	Yield (mg/L)
2551_01_A12	3	100.0	1.48	18.1
2554_01_D11	1	94.8	1.48	47.1
2558_02_G09	1	95.6	1.48	38.5
2551_01_B11	1	96.2	1.50	30.4
2555_01_A04	1	100.0	1.47	25.8
2555_01_A01	1	96.7	1.47	45.4
368_01_C05	0	97.5	1.45	30.0
2552_02_B02	32	100.0	1.82	22.6

125
126 Analysis of the antibody sequences revealed that the six affinity matured antibodies had
127 light chains belonging to two different germlines, germline IGLV3-21 for 2551_01_B11,
128 2555_01_A01, 2555_01_A04, and 2558_02_G09 and germline IGLV6-57 for 2551_01_A12 and
129 2554_01_D11. The parental antibody had germline IGLV6-57, meaning that two of the six affinity
130 matured antibodies had light chains belonging to the same germline as the parental antibody. From
131 the comparison of the three light chain CDR regions of the antibodies presented in Fig. 1C, it could
132 also be seen that for the two antibodies maintaining the parental germline, the CDR-L2 was
133 identical to the parental, whereas the CDR-L1 and CDR-L3 had 2-3 amino acid differences. For

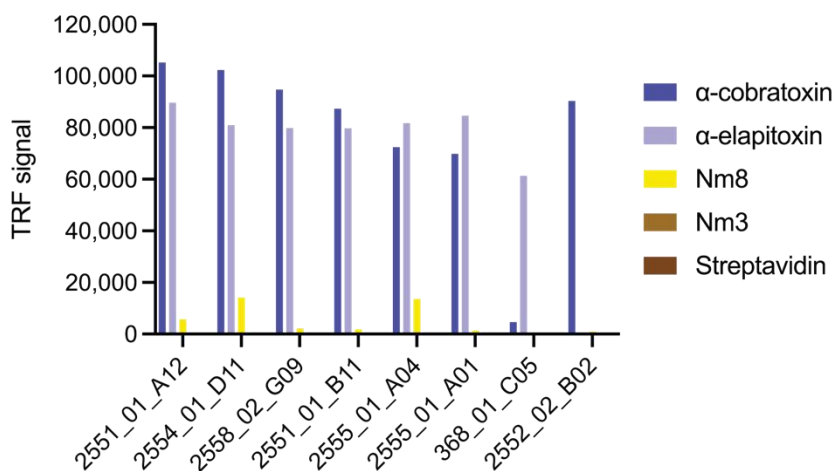
134 the remaining four antibodies with different light chain germline, all V_L CDR sequences were
135 significantly different from the parent antibody sequence.

136 To evaluate if the light-chain-shuffling campaign generated antibodies with improved
137 affinity, surface plasmon resonance (SPR) was used to determine the affinity of the top six
138 antibodies as well as the parental antibody. To this purpose, all antibodies were reformatted to the
139 monovalent Fab format to measure 1:1 binding kinetics of each antibody against both α -cobratoxin
140 and α -elapitoxin (for SPR sensograms see Fig. S1). Data showed that all six antibodies displayed
141 higher affinity to both toxins as compared to the parental antibody (Table 2). The largest
142 improvement was observed for 2551_01_A12 and 2554_01_D11 (32 and 50-fold improvement of
143 binding to α -cobratoxin and 13 and 8-fold improvement of binding to α -elapitoxin, respectively),
144 providing both antibodies with low single-digit nanomolar affinities to both toxins. Thus, a
145 significant improvement in both affinity and cross-reactivity was observed. Antibodies
146 2551_01_A12 and 2554_01_D11 were selected for further characterization based on affinity,
147 cross-reactivity, expression yield, and developability data.

A



B



C

Antibody ID	Gene	CDR-L1	CDR-L2	CDR-L3
368_01_C05	IGLV6-57	SGSIA STY	EDN	Q SYDSSNGSVV
2551_01_A12	IGLV6-57	SGRIV SDY	EDN	Q SYDSSNAYVV
2554_01_D11	IGLV6-57	SGSIGSDY	EDN	Q SYDRSNHEVV
2551_01_B11	IGLV3-21	- - NIGSNI	HNT	QVWDSSEHVV
2555_01_A01	IGLV3-21	- - NIGQQI	SDS	QVWDSGSDHV
2555_01_A04	IGLV3-21	- - YIGGES	DDT	QVWDVSSSDHV
2558_02_G09	IGLV3-21	- - NIGQQI	DGS	QVWDITSDHV

148

149 **Fig. 1. Cross-panning selection strategy as well as assay and sequence data for selected IgGs.**

150 A) Selection strategy illustrating how cross-panning was performed, including antigen
 151 concentrations. B) ENC DELFIA showing cross-reactivity of top six affinity matured IgGs
 152 (2551_01_A12, 2551_01_B11, 2554_01_D11, 2555_01_A01, 2555_01_A05, and 2558_02_G09)
 153 in comparison with parental IgG (368_01_C05) and clone 2552_02_B02 from a previously

154 published study⁸. C) Comparison of CDR-L, CDR-L2, and CDR-L3 sequences for the top six
155 chain-shuffled antibodies and the parental antibody.

156 **Table 2. Affinity measurements using Surface Plasmon Resonance (SPR).** SPR was used to
157 measure the affinity of the top six chain-shuffled antibodies (2551_01_A12, 2551_01_B11,
158 2554_01_D11, 2555_01_A01, 2555_01_A05, and 2558_02_G09) and the parental antibody
159 (368_01_C05) in the Fab format to both α -cobratoxin and α -elapitoxin. The dissociation constants,
160 on-rates, and off-rates are provided. For sensograms see Fig. S1.

Antibody ID	α -cobratoxin			α -elapitoxin		
	K _D (nM)	k _{on} (M·s)	k _{off} (s ⁻¹)	K _D (nM)	k _{on} (M·s)	k _{off} (s ⁻¹)
2551_01_A12	2.79	$1.80 \cdot 10^5$	$5.02 \cdot 10^{-4}$	1.12	$1.25 \cdot 10^5$	$1.40 \cdot 10^{-4}$
2554_01_D11	1.78	$1.28 \cdot 10^5$	$2.29 \cdot 10^{-4}$	1.69	$1.05 \cdot 10^5$	$1.77 \cdot 10^{-4}$
2558_02_G09	2.77	$2.14 \cdot 10^5$	$5.94 \cdot 10^{-4}$	3.04	$1.39 \cdot 10^5$	$4.22 \cdot 10^{-4}$
2551_01_B11	4.27	$1.17 \cdot 10^5$	$5.00 \cdot 10^{-4}$	2.87	$6.37 \cdot 10^5$	$1.83 \cdot 10^{-4}$
2555_01_A04	7.46	$2.22 \cdot 10^5$	$1.65 \cdot 10^{-3}$	2.21	$9.26 \cdot 10^5$	$2.05 \cdot 10^{-4}$
2555_01_A01	8.41	$2.02 \cdot 10^5$	$1.70 \cdot 10^{-3}$	1.81	$1.00 \cdot 10^5$	$1.81 \cdot 10^{-4}$
368_01_C05	89.6	$1.83 \cdot 10^4$	$1.64 \cdot 10^{-2}$	14.3	$6.47 \cdot 10^4$	$9.25 \cdot 10^{-4}$

161 162 Because the binding profiles of the cross-reactive antibodies derived from antibody 368_01_C05
163 were significantly different from antibody 2552_02_B02, SPR was used to determine if the
164 antibodies bound the same or overlapping epitopes on α -cobratoxin (see Fig. S2). Using
165 2554_01_D11 as a representative of the cross-reactive antibodies, this study revealed that neither
166 of the two antibodies 2552_02_B02 or 2554_01_D11 could bind α -cobratoxin if the other antibody
167 was already bound to the toxin, suggesting that the antibodies recognized the same or overlapping
168 epitopes.

169 **Native mass spectrometry reveals cross-reactivity to several toxins from elapid snakes of**
170 **three different genera**

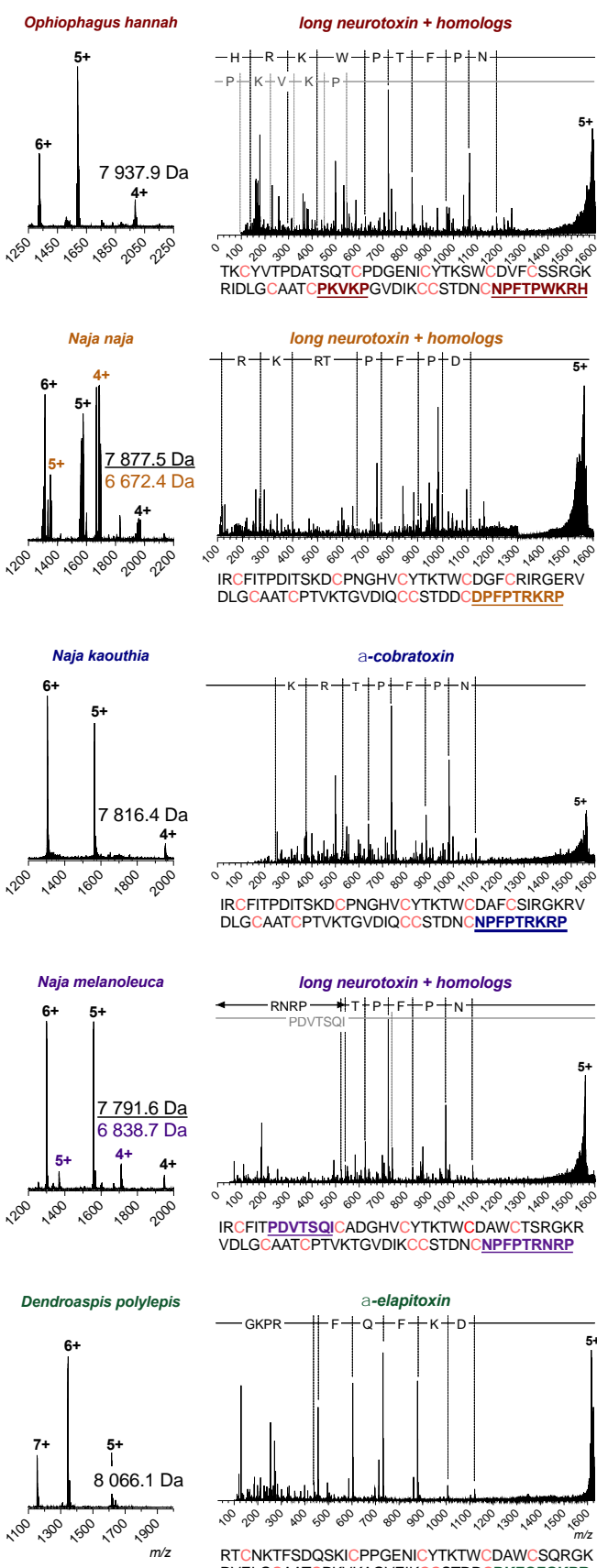
171 To further explore the cross-reactivity of the discovered antibodies, IgG 2554_01_D11 was tested
172 for its binding to toxins in five whole venoms including *N. kaouthia*, *N. melanoleuca*, *N. naja*,
173 *Ophiophagus hannah*, and *D. polylepis*. These venoms from African (*D. polylepis* and *N.*
174 *melanoleuca*) and Asian (*N. kaouthia*, *N. naja* and *O. hannah*) snakes all possess a relatively high
175 content of long chain α -neurotoxins, ranging from 13.2% for *D. polylepis*¹⁸ to 55% for *N.*
176 *kaouthia*¹⁷, except *N. naja* that has been reported to have a long chain α -neurotoxin-content of
177 about 2-5%²⁶. For this purpose, native mass spectrometry (MS), was used to investigate the
178 interactions between the antibody and toxins from the four snake venoms.

179 Prior to native mass spectrometry analysis, the venoms and the IgG were fractionated using
180 SEC (Fig. S3). The IgG was mixed with each of the SEC-generated toxin fractions, before analysis
181 using native MS to determine binding (Fig. S3). This analysis revealed that 2554_01_D11 only
182 bound toxins of masses in the range expected for the group of three-finger toxins (3FTx) to which
183 all α -neurotoxins belong. To identify the toxins, the toxin:antibody complexes were isolated using
184 MS/MS and subjected to collisional dissociation to eject the toxins from the antibody, allowing
185 their intact mass to be determined. The primary dissociation product from these experiments were
186 proteins of masses between 7,800 and 8,200 Da, corresponding to typical masses of long chain α -
187 neurotoxins (Fig. 2).

188 The sequences of the toxins bound by 2554_01_D11 were investigated via top-down
189 proteomics to confirm the identities of these toxins. For these experiments, the toxin:antibody
190 complexes were purified using SEC. Toxins were dissociated from the antibody by applying a high
191 cone voltage. This is a focusing voltage applied to the cone, which is located in the source region

192 of the instrument. Increasing this voltage leads to harsh condition that can dissociate noncovalent
193 complexes. Since this dissociation occurs before the quadrupole, the most prominent charge state
194 of each ejected toxin could then be isolated using MS/MS for top-down sequencing. This isolation
195 is important, as it ensures that the peptide fragmentation peaks only correspond to the toxin of
196 interest. For the toxins of masses between 7,800 and 8,200 Da, only one readily discernible peptide
197 fragment series was detected for each precursor ion. The limited amount of sequence data obtained
198 from these experiments is attributed to the presence of disulfide bonds present in snake venom
199 toxins, which cannot be broken using this fragmentation technique²⁷⁻²⁹.

200 A BLAST search against all available elapid protein sequences revealed that the peptide
201 sequences obtained by top-down analysis were unique to long chain α -neurotoxins and that each
202 peptide only had one complete match to long chain α -neurotoxins homologs from the investigated
203 venom. Sequence data combined with the detected masses of the toxins revealed that
204 2554_01_D11 was capable of binding to long chain α -neurotoxin-containing SEC fractions across
205 all tested venoms. This suggested that this antibody is cross-reactive against long chain α -
206 neurotoxins present in all five tested venoms, further highlighting the broadly cross-reactive
207 behavior of 2554_01_D11.



209 **Fig. 2. Intact masses and top-down sequence analysis of toxins bound by 2554_01_D11.**

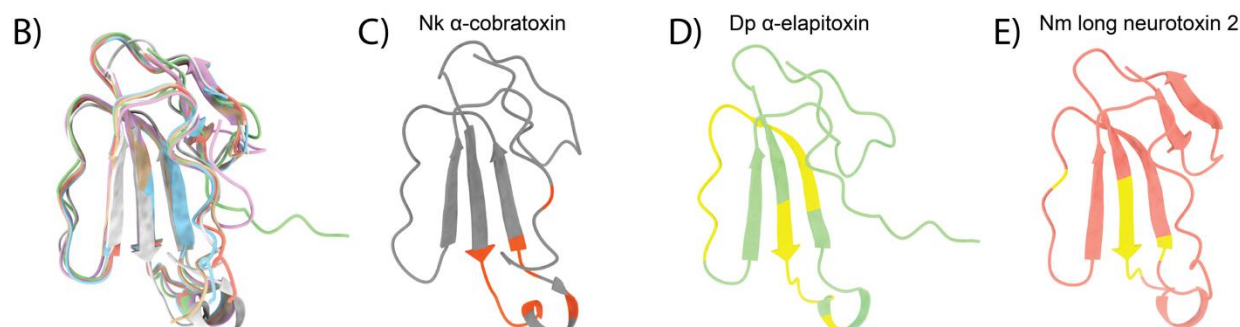
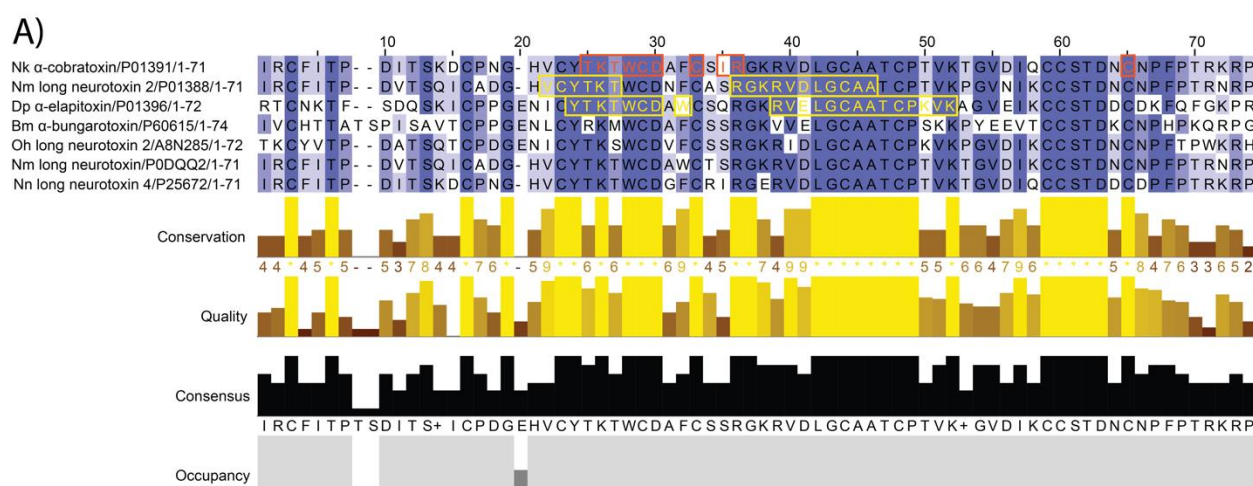
210 Names above the mass spectra have been color-coded for each species as follows; *O. hannah* (red),
211 *N. naja* (orange), *N. kaouthia* (blue), *N. melanoleuca* (purple) and *D. polylepis* (green). The spectra
212 on the left-hand side show the charge state distribution for the toxins ejected from the antibody
213 complex by applying a high cone voltage, where the masses of the identified toxins are given in
214 Daltons. The top-down sequence spectra for the most prominent charge state of each toxin are
215 shown in the right-hand side. The difference in *m/z* are outlined via dotted lines on top and match
216 the specific amino acid or peptide. The full amino acid sequence for the proposed identity of the
217 toxins is given below each spectrum, with the matching peptides found during the top-down
218 analysis colored and underlined. Cysteines in the sequence are colored pink.

219

220 The toxin homologs specifically identified to be bound by 2554_01_D11 were long
221 neurotoxin 2 (A8N285) from *O. hannah*, α -cobratoxin (P01391) from *N. kaouthia*, long neurotoxin
222 2 (P01388) and long neurotoxin (P0DQQ2) from *N. melanoleuca*, long neurotoxin 4 (P25672)
223 from *N. naja*, and α -elapitoxin (P01396) from *D. polylepis*. In addition, the antibody was shown
224 to bind α -bungarotoxin (P60615) from *B. multicinctus* using SPR (data not shown). The average
225 sequence similarity of the seven toxins was 62% (stdev: 9.9%), with an identity of 38% across all
226 toxins; a total of 28 amino acid positions were identical across all toxins (Fig. 3A). The highest
227 identity was observed between α -cobratoxin and long neurotoxin 2 from *N. melanoleuca* (83%)
228 and the lowest identity was observed between long neurotoxin 2 from *N. melanoleuca* and α -
229 bungarotoxin (51%). Additionally, a structural comparison was performed via root-mean-square
230 deviation (RMSD) and revealed a mean pruned/total similarity of 0.81 \AA /3.1 \AA (stdev:
231 0.26 \AA /1.23 \AA), respectively; the best match appeared to be between long neurotoxin and long

232 neurotoxin 2 from *N. melanoleuca* (0.23Å/0.23Å) and the worst match appeared to be between
233 long neurotoxin 2 from *O. hannah* and α -cobratoxin (pruned: 1.18Å) and α -elapitoxin and α -
234 bungarotoxin (total: 4.5Å; Fig 3B). For α -cobratoxin, the amino acid residues involved in binding
235 to the nicotinic acetylcholine receptor have been highlighted both in the sequence (Fig. 3A) and in
236 the structure on the toxin (Fig. 3C). Additionally, the residues that through a high-density peptide
237 microarray-based study³⁰ have been identified to be involved in the binding between antivenom-
238 derived antibodies and α -elapitoxin and long neurotoxin 2 from *N. melanoleuca*, respectively, have
239 been highlighted in the toxin sequence in Fig. 3A and in the toxin structure in Fig. 3D and 3E.

240



242 **Fig. 3. Alignment and epitope identification of all investigated long chain α -neurotoxins, i.e.**
243 **α -cobratoxin (P01391/1CTX) from *N. kaouthia*, α -elapitoxin (P01396/AF-P01396) from *D.***

244 ***polylepis*, α -bungarotoxin (P60615/1HC9) from *B. multicinctus*, long neurotoxin 2**
245 **(A8N285/AF-A8N285) from *O. hannah*, and long neurotoxin (P0DQQ2), long neurotoxin 4**
246 **from *N. naja* (P25672/AF-P25672), and long neurotoxin 2 (P01388/AF-P01388) from *N.***
247 ***melanoleuca*.** A) Sequence alignment using Clustal Omega with boxes indicating residues
248 involved in binding to the nicotinic acetylcholine receptor (orange) or bound by antivenom
249 antibodies (yellow). B) Structural alignment in ChimeraX with the following colors representing
250 each toxin: orange (long neurotoxin 2 from *N. melanoleuca*), beige (long neurotoxin 2 from *O.*
251 *hannah*), purple (α -bungarotoxin), green (α -elapitoxin from *D. polylepis*), blue (long neurotoxin 4
252 from *N. naja*), and grey (α -cobratoxin from *N. kaouthia*). C) Amino acid residues on α -cobratoxin³¹
253 known to be involved in binding to its native target, *i.e.*, the nicotinic acetylcholine receptor³¹
254 (orange). D) Amino acid residues in α -elapitoxin suggested to be bound by antivenom antibodies
255 based on high-density peptide microarray analysis³⁰ (yellow). E) Amino acid residues in long
256 neurotoxin 2 from *N. melanoleuca* suggested to be bound by antivenom antibodies based on high-
257 density peptide microarray analysis³⁰ (yellow).

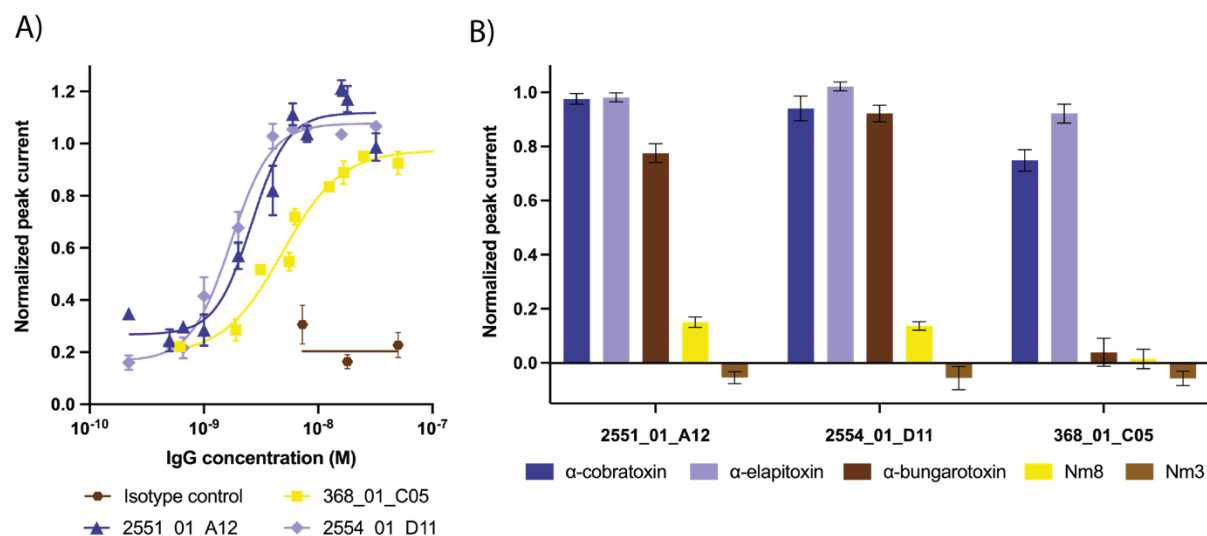
258 **Increased *in vitro* neutralization potency and broadening of cross-neutralization**

259 After having established the broadly cross-reactive nature of one of the top two chain-shuffled
260 antibodies (2554_01_D11), automated patch-clamp technology was applied to assess if binding
261 translated into functional neutralization *in vitro* for 2551_01_A12 and 2554_01_D11, as well as
262 for the parental clone, 368_01_C05. Here, a human derived cell line endogenously expressing the
263 nAChR was used for measuring the acetylcholine-dependent current. α -cobratoxin inhibited this
264 current in a concentration-dependent manner, and the IC₈₀ value for the toxin was determined.
265 Thereafter, the concentration-dependent neutralization of the current-inhibiting effect of α -
266 cobratoxin by the three antibodies was determined. Results demonstrated that all three antibodies

267 were able to fully neutralize the effects of α -cobratoxin, whereas an irrelevant isotype control
268 antibody (recognizing a dendrotoxin) had no effect (Fig. 4A). The parental antibody, 368_01_C05
269 neutralized α -cobratoxin mediated inhibition of acetylcholine-dependent currents with an EC₅₀
270 value of 4.9 nM and relatively shallow concentration-response curve slope. In contrast, the
271 optimized antibodies, 2551_01_A12 and 2554_01_D11 exhibited improved EC₅₀ values of 2.6
272 nM and 1.7 nM respectively with steeper slopes for the concentration-response curves. These EC₅₀
273 values translate into toxin:antibody molar ratios of 1:1.23 for 368_01_C05, 1:0.65 for
274 2551_01_A12, and 1:0.43 for 2554_01_D11. Since each IgG has two binding sites, the
275 theoretically lowest amount of IgG needed to neutralize the effect of one toxin would be 0.5 IgGs.

276 To determine if the increased cross-reactivity to other α -neurotoxins translated into cross-
277 neutralization, a single concentration antibody screen was set up using the Qube 384 system. Here,
278 the three antibodies (368_01_C05, 2551_01_A12, and 2554_01_D11) were tested against α -
279 cobratoxin from *N. kaouthia*, α -elapitoxin from *D. polylepis*, and Nm8 from *N. melanoleuca*,
280 which all were toxins that 2554_01_D11 had been shown to bind through native MS. In addition,
281 α -bungarotoxin was included, as it has 58% sequence identity to α -cobratoxin, is commercially
282 available, and is an important toxin to neutralize in the venom of *B. multicinctus*. As a control,
283 Nm3, a venom fraction from *N. melanoleuca* containing a short chain α -neurotoxin that also binds
284 to the nAChR, but is not bound by any of the three antibodies, was included. This automated patch-
285 clamp screening revealed that α -cobratoxin and α -elapitoxin could be neutralized by all three
286 antibodies in this assay (Fig. 4B). Additionally, the chain-shuffled clones were able to neutralize
287 α -bungarotoxin and partially neutralize the α -neurotoxins present Nm8, none of which was
288 achieved by the parental clone. Collectively, the results of the *in vitro* neutralization assays using
289 automated patch-clamp demonstrated that the chain-shuffled antibodies were both more potent in

290 their neutralization of α -cobra toxin, as well as more broadly neutralizing than the parental
291 antibody, inhibiting the effect of α -neurotoxins from snakes of three different genera inhabiting
292 both Asia and Africa. Based on binding, developability, affinity, expression, and *in vitro*
293 neutralization data, 2554_01_D11 was selected as the top candidate for *in vivo* testing.



294

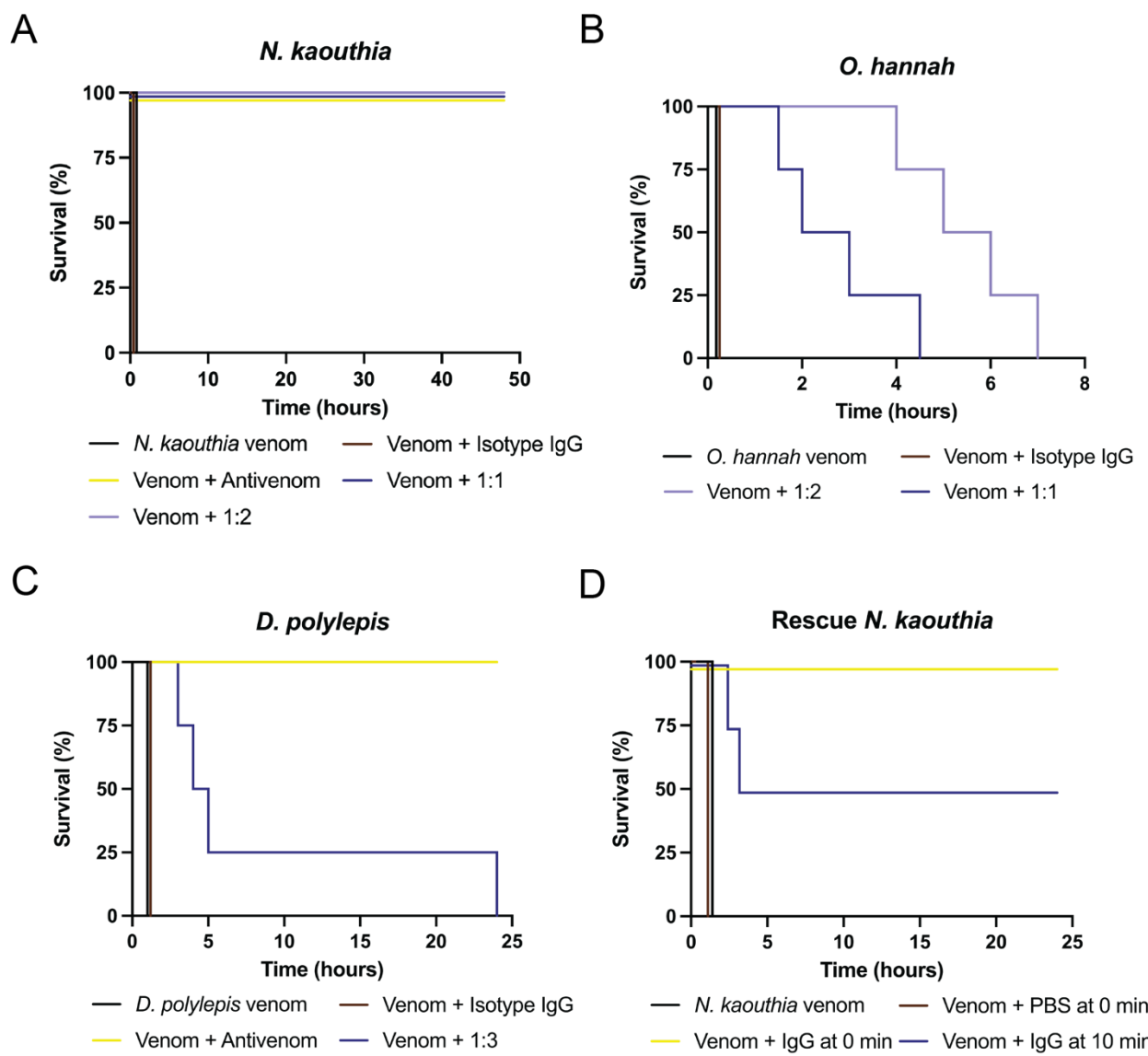
295 **Fig. 4. Electrophysiological determination of the *in vitro* cross-neutralizing potential of**
296 **2551_01_A12, 2554_01_D11, and 368_01_C05.** Automated patch-clamp experiments were
297 performed to determine the ability of the antibodies to prevent the current-inhibiting effect that α -
298 neurotoxins exert on the nAChR. A) Concentration-response curves illustrating how increasing
299 concentrations of the three antibodies prevent nAChR blocking by α -cobra toxin. B) Single
300 concentration plot outlining the cross-neutralizing potential of the antibodies against α -cobra toxin
301 from *N. kaouthia*, α -elapitoxin from *D. polylepis*, α -bungarotoxin from *B. multicinctus*, and Nm8
302 from *N. melanoleuca*. In addition, a negative control Nm3, a fraction from *N. melanoleuca* venom
303 containing a short α -neurotoxin, was included. The toxin to antibody molar ratios used were 1:22
304 for α -cobra toxin, 1:40 for α -elapitoxin, 1:5 for α -bungarotoxin, 1:2.3 for Nm8, and 1:3.2 for Nm3.

305 ***In vitro* neutralization data translates to complete or partial *in vivo* neutralization of snake
306 venoms from different genera and continents**

307 To verify that the *in vitro* cross-neutralization potential of 2554_01_D11 translated into *in vivo*
308 cross-neutralization, animal experiments were set up to evaluate the ability of the antibody to
309 prevent or delay venom-induced lethality. Here, snake venoms from three different species
310 belonging to three genera, one from Africa, *i.e.* *D. polylepis*, and two from Asia, *i.e.* *N. kaouthia*
311 and *O. hannah*, were included. Notably, each of these venoms contain a substantial amount of long
312 chain α -neurotoxins (a relative abundance of 13.2%¹⁸, 55%¹⁷, and ~20%³², respectively). Two
313 LD₅₀s of each venom were preincubated with 2554_01_D11 in a 1:1 and 1:2 toxin:antibody molar
314 ratio for *N. kaouthia* and *O. hannah* or a 1:3 toxin:antibody molar ratio for *D. polylepis* before
315 being administered i.v. to the mice. As controls, mice were injected with venom alone, venom
316 preincubated with commercial antivenoms (except in the case of *O. hannah*, where no antivenom
317 was available), or venom preincubated with an antibody isotype control.

318 Results of the studies demonstrated that all mice in the venom only control group, as well
319 as the mice receiving venom preincubated with the isotype control antibody, died within the first
320 hour after the challenge, with evident signs of limb paralysis and respiratory difficulty. As
321 expected, mice receiving *N. kaouthia* or *D. polylepis* venoms preincubated with commercially
322 available antivenoms survived for the entire observation period, and no signs of neurotoxicity were
323 observed. In experiments where mice were injected with venoms incubated with 2554_01_D11,
324 results varied depending on the venom. In the case of *N. kaouthia* venom, complete neutralization
325 was observed at both toxin:antibody molar ratios, since mice survived during the 48-hour
326 observation time. Moreover, mice did not show any signs of neurotoxicity, *i.e.*, limb paralysis or
327 respiratory difficulty along the whole period. In the case of *O. hannah*, there was a dose-dependent

328 delay in the time of death, as compared to controls receiving venom alone. Likewise, a delay in
329 the time of death was observed in the case of *D. polylepis* venom (Fig 5).



330

331 **Fig. 5. Kaplan-Meier survival curves for the antibody 2554_01_D11.** A), B), and C) Mixtures
332 containing 2 LD₅₀s of venom of either *N. kaouthia*, *O. hannah*, or *D. polylepis* were preincubated
333 with the antibody, 2554_01_D11, at various toxin:antibody ratios and then administered i.v. to
334 groups of four mice. Controls included mice receiving venom alone or venom incubated with either
335 an irrelevant isotype antibody control or a commercial horse-derived antivenom. Signs of toxicity

336 were observed, and deaths were recorded for a maximum period of 48 hours. D) 2 LD₅₀s *N.*
337 *kaouthia* venom was administered s.c. following i.v. administration of IgG 2554_01_D11 either
338 immediately following venom administration or 10 minutes after venom administration. As a
339 control, mice were administered venom s.c. and PBS i.v. Signs of toxicity were observed, and
340 deaths were recorded for 24 hours. Mice receiving antibody immediately following venom
341 administration had a dose of 1:2.5 toxin to antibody molar ratio while mice receiving antibody 10
342 minutes post venom administration had an antibody dose of 1:2 toxin to antibody molar ratio.

343
344 Next, the ability of the antibody to abrogate lethality of *N. kaouthia* venom in rescue-type
345 experiments was assessed. For this, the subcutaneous (s.c.) route of venom injection was used in
346 order to better reproduce the actual circumstances of envenoming. The estimated LD₅₀ by the s.c.
347 route was 10.3 µg (95% confidence interval: 5.0 – 16.8 µg). Mice were challenged by the s.c. route
348 with a dose of venom corresponding to 2 LD₅₀s, *i.e.*, 20 µg, followed by the i.v. administration of
349 the 2554_01_D11 antibody in a volume of 100 µL, at a molar ratio of 1:2.5 (toxin:antibody).
350 Control mice injected with venom only died within 40 – 60 min, with evident signs of limb and
351 respiratory paralysis. When the antibody was administered immediately after venom injection, all
352 mice survived the 24-hour observation period and did not show any evidence of limb or respiratory
353 paralysis. When the antibody was provided 10 min after venom injection, two out of four mice
354 died, but there was a delay in the time of death (150 min and 180 min). The other two mice survived
355 the 24-hour observation time and did not show signs of paralysis (Fig 5D).

356
357

358 **DISCUSSION**

359 Here, we demonstrate that an antibody discovered from a naïve human library with limited cross-
360 reactivity to other α -neurotoxins and without the ability to prevent lethality induced by α -
361 cobra toxin in mice, can be improved by light chain-shuffling, resulting in enhanced affinity,
362 potency, and cross-neutralization capacity.

363 The most promising antibody we discovered, 2554_01_D11, bound seven long chain α -
364 neurotoxins arising from five snakes of four genera distributed across both Asia and Africa.
365 Notably, cross-reactive binding was detected despite sequence alignment of the seven α -
366 neurotoxins revealing substantial differences in sequence identity, with an overall identity of only
367 31%. This is likely due to the fact that, despite the low overall identity, a total of 29 positions in
368 the toxin sequences contain identical amino acids across all seven α -neurotoxins, including most
369 of the residues previously identified as playing a significant role in the binding between α -
370 cobra toxin/ α -bungarotoxin and the nAChR³¹. Specifically, these amino acid residues include
371 Trp25, Cys26, Asp27, Ala28, Phe29, Cys30, Arg33, Lys35, and Arg36/Val39 (α -cobra toxin/ α -
372 bungarotoxin) on loop II and Phe65/Val39 (α -cobra toxin/ α -bungarotoxin) on the C-terminus,
373 where a single mutation of one of these residues has been shown to cause a more than five-fold
374 decrease in affinity to the nAChR³³. Furthermore, high-density peptide microarray analysis
375 previously suggested that positions 22-27 and 36-46 represent linear B-cell epitopes for antibodies
376 to long neurotoxin 2 from *N. melanoleuca*, recognized by one of the most effective antivenoms
377 available (SAIMR, produced by SAVP), like positions 24-30, 32, and 39-50 do for α -elapitoxin³⁰.
378 This emphasizes the potential importance of Trp25, Cys26, Asp27, Ala28, Phe29, Cys30, and
379 Arg36 for the ability of antibodies to recognize this toxin. Together, this presents a plausible
380 explanation for the broad cross-reactivity we observed for 2554_01_D11 and indicates the

381 importance of epitope similarity (as opposed to overall sequence identity) in the pursuit of cross-
382 reactive antibodies⁴. However, the boundaries of the cross-reactivity of 2554_01_D11 have not
383 been established in this study, as all long chain α -neurotoxins investigated were recognized by the
384 antibody. Future work aiming to investigate the boundaries of cross-reactivity could include testing
385 the antibody for binding to long chain α -neurotoxins from other snakes, such as *B. candidus*³⁴, *B.*
386 *fasciatus*³⁴, or *N. haje legionis*³⁵. Such studies could potentially provide general cues to how
387 antibody cross-reactivity can be optimized for antibodies targeting toxins and similar antigens.

388 Besides cross-reactive binding, we also demonstrated the broad neutralizing potential of
389 2554_01_D11. *In vivo* studies showed that lethality induced by three snake venoms of different
390 genera distributed across both Asia and Africa was either prevented or delayed by the antibody,
391 2554_01_D11. For *N. kaouthia* venom, the antibody was able to completely prevent lethality in
392 envenomed mice with no signs of neurotoxicity even at the lowest tested toxin:antibody molar
393 ratio of 1:1. Moreover, this antibody was able to neutralize lethality induced by the venom of *N.*
394 *kaouthia* in rescue-type experiments, which more closely resemble the actual circumstances of
395 envenoming³⁶. Complete neutralization was achieved when the antibody was administered
396 immediately after the venom challenge, and even after a delay of 10 min between venom and
397 antibody administration, 2 out of 4 mice survived and death was delayed in the other two.

398 Despite the antibody 2554_01_D11 possessing very similar affinities to α -cobratoxin and
399 α -elapitoxin from *D. polylepis*, the antibody was unable to prevent lethality induced by *D.*
400 *polylepis* venom, even at the tested toxin:antibody molar ratio of 1:3. Survival was, however,
401 prolonged several hours, suggesting that the antibody did provide partial neutralization of the
402 venom. These results are perhaps not surprising, as the venom of *D. polylepis* is more complex
403 than that of *N. kaouthia*, and it is well-established that toxins other than long chain α -neurotoxins

404 (i.e. short chain α -neurotoxins and dendrotoxins) play important roles for the toxicity of *D.*
405 *polylepis* venom¹⁸. Where lethality of *N. kaouthia* venom is mainly attributed to the high content
406 of long chain α -neurotoxins, the short chain α -neurotoxins present in *D. polylepis* venom have
407 been estimated to contribute with about a third of the toxicity of the venom¹⁸. Thus, even if all
408 long chain α -neurotoxins were neutralized in the venom, neutralization of short chain α -
409 neurotoxins and possibly even dendrotoxins could still be necessary to prevent venom-induced
410 lethality. As the affinity of the antibody to α -elapitoxin was almost identical to that of α -cobratoxin,
411 we speculate that the antibody, 2554_01_D11, might be able to neutralize the effects of the long
412 chain α -neurotoxins from *D. polylepis*, but that the mice eventually die due to lethality induced by
413 short chain α -neurotoxins and possibly dendrotoxins. Similarly, the lethal effects of the venom of
414 *O. hannah* were only delayed, probably since this venom also consists of a mixture of both long
415 and short chain α -neurotoxins.

416 In this study, monoclonal IgG antibodies with broad cross-reactivity to different long chain
417 α -neurotoxins were discovered, and an epitope binning study revealed that the cross-reactive
418 antibody 2554_01_D11 bound the same or an overlapping epitope to the previously reported
419 antibody 2552_02_B02, which only recognizes α -cobratoxin⁸. In the future, determination of the
420 structure of the two antibodies in complex with α -cobratoxin might provide further insight into
421 how two antibodies binding to the same or overlapping epitope with similar affinity can display
422 such different levels of cross-reactivity.

423 When comparing the neutralizing capacities of the two antibodies, 2554_01_D11 and
424 2552_02_B02, another noteworthy observation emerges. Antibody 2554_01_D11 possessed
425 significantly higher efficacy in neutralizing *N. kaouthia* venom *in vivo* when compared to what
426 was reported for 2552_02_B02⁸. Where 2554_01_D11 neutralized all signs of neurotoxicity at the

427 lowest tested dose of 1:1 toxin to antibody molar ratio, 2552_02_B02 only prevented lethality
428 induced by *N. kaouthia* venom in 3 out of 4 mice at a 1:4 molar ratio, with mice showing clear
429 signs of neurotoxicity. These results were especially remarkable, as the two antibodies performed
430 similarly both in electrophysiological *in vitro* neutralization assays and had similar affinities to α -
431 cobra toxin (490 pM for 2552_02_B02 and 1.78 nM for 2554_01_D11). Except for the difference
432 in cross-reactivity profiles, the only significant difference between the two antibodies was in their
433 developability profiles. In these developability assessment assays, 2554_01_D11 performed
434 similarly to Aliricumab (control for good developability), whereas 2552_02_B02 performed
435 comparably to Bococizumab (control for poor developability)²⁵. It is thus possible that this
436 difference in self-association and interaction with the SEC column seen in these assays may
437 correlate with different pharmacokinetic or pharmacodynamic properties of the two antibodies,
438 which could explain their contrasting performance *in vivo*. This thus suggests that detailed
439 developability characterization should be included as part of early discovery to maximize the *in*
440 *vivo* efficacy and clinical success of recombinant antivenoms.

441 In conclusion, this study demonstrates the utility of combining cross-panning strategies in
442 phage display with affinity maturation using chain-shuffling for the development of high-affinity
443 human monoclonal IgG antibodies that show broadly-neutralizing effects against neurotoxic elapid
444 snake venoms *in vitro* and *in vivo*. Such antibodies might be useful for designing future
445 envenoming therapy, but more importantly, the pipeline presented here could also be exploited for
446 the development of broadly-neutralizing antibodies against other targets of medical importance.
447 These targets could include toxins from other venomous animals than snakes, but also
448 hypervariable and mutating antigens from infectious bacteria, viruses, and parasites, or even
449 neoepitopes in non-infectious diseases.

450 **MATERIALS AND METHODS**

451 **Toxin preparation**

452 α -cobratoxin (L8114), α -bungarotoxin (L8115), and whole venoms from *N. kaouthia* (L1323), *N.*
453 *melanoleuca* (L1318), *D. polylepis* (L1309), and *O. hannah* (L1357) were obtained from Latoxan
454 SAS, France. Venom fractions containing long α -neurotoxins (Dp7 from *D. polylepis* and Nm8
455 from *N. melanoleuca*) were isolated from crude venom by fractionation using RP-HPLC (Agilent
456 1200). Venoms were fractionated using a C18 column (250 \times 4.6 mm, 5 μ m particle; Teknokroma)
457 and elution was carried out at 1 mL/min using Solution A (water supplemented with 0.1% TFA)
458 and a gradient towards solution B (acetonitrile supplemented with 0.1% TFA): 0% B for 5 min,
459 0–15% B over 10 min, 15–45% B over 60 min, 45–70% B over 10 min, and 70% B over 9 min^{18,24}.
460 Fractions were collected manually and evaporated using a vacuum centrifuge. Toxins were
461 dissolved in phosphate buffered saline (PBS) and biotinylated using a 1:1 (toxin:biotinylation
462 reagent) molar ratio for α -cobratoxin and 1:1.5 molar ratio for the remaining toxins as described
463 elsewhere⁶. Following biotinylation, toxins were purified as well as the degree of biotinylation was
464 determined as previously described⁸.

465 **Library generation using chain-shuffling**

466 Light chain-shuffled libraries containing the heavy chain of antibody 368_01_C05 were created as
467 described previously⁸. Two libraries were created, one with kappa and one with lambda light
468 chains. The size of the kappa library was 1.67×10^8 whereas the lambda library was 1.01×10^8 .
469 Colony PCR revealed 96% of the transformants to have successful heavy chain ligation.

470

471

472 **Library rescue, solution-based phage display selection, and polyclonal DELFIA**

473 Phages were rescued from the light chain-shuffled libraries and three rounds of selections were
474 performed as described elsewhere³⁷ with a few exceptions. Phages were not concentrated using
475 PEG precipitation, but instead phage-containing supernatants were blocked in PBS supplemented
476 with Milk Protein (MPBS) and used directly for selections. Additionally, deselection of
477 streptavidin-specific phages was performed as described previously⁸. Lastly, to obtain scFvs with
478 high affinity and broad cross-reactivity to different long α -neurotoxins cross-panning between α -
479 cobra toxin and Dp7 was performed as previously described⁷ as well as antigen concentrations were
480 lowered between each round of selection starting at 10 nM and ending at 4 pM. The kappa and
481 lambda libraries were mixed before the first round of selections. To assess the polyclonal output
482 of the selections a polyclonal DELFIA was performed determining binding to both α -cobra toxin,
483 Dp7, and MPBS.

484 **Subcloning, screening, and sequencing of scFvs**

485 The genes encoding the scFvs from five of the obtained selection outputs (representing different
486 cross-panning strategies) were subcloned into the pSANG10-3F expression vector to allow for
487 monoclonal screening of the clones as described elsewhere⁶. Briefly, scFv-encoding genes from
488 five selected output phage libraries were amplified using primers M13leadseq
489 (AAATTATTATTCGCAATTCTTGGTTGTCCT) and Notmycseq
490 (GGCCCCATTCAAGATCCTCTTGAGATGAG) before restriction using *Nco*I and *Not*I
491 restriction endonuclease sites. The genes were ligated into pSANG10-3F and transformed into *E.*
492 *coli* strain BL21 (DE3) (New England Biolabs). From each selection output 184 clones were
493 selected and expressed in 96-well plates. The scFvs were evaluated for their binding to α -
494 cobra toxin, Dp7, streptavidin, and milk protein using a monoclonal DELFIA assay as described

495 previously⁸. From this, 329 clones were cherry-picked and sequenced (Eurofins Genomics
496 sequencing service) using S10b primer (GGCTTGTTAGCAGCCGGATCTCA). The antibody
497 frameworks and the CDR regions of the light chains were annotated using Geneious Biologics
498 (Biomatters), and 67 clones were identified as unique based on light chain CDR3 regions.

499 **Reformatting to IgG and Fab format**

500 A total of 62 clones were selected for reformatting into the fully human IgG1 and Fab format. The
501 reformatting into the IgG1 format was completed as described in Laustsen *et al.*⁶, whereas
502 reformatting into the Fab format was completed as described in Ledsgaard *et al*⁸. The binding of
503 the IgGs to α -cobratoxin, Dp7, Nm8, and streptavidin was assessed and ranked using an
504 expression-normalized capture (ENC) assay described previously⁸.

505 **Developability characterization**

506 To aid in the selection of the top antibody candidates for further characterization, the biophysical
507 behavior of the 62 reformatted clones in the IgG format was characterized using HPLC-SEC and
508 AC-SINS. For HPLC-SEC, the purified antibodies were loaded onto a Superdex 200 Increase
509 5/150 column at a flow rate of 0.25 mL/min using an Agilent 1100 HPLC instrument. AC-SINS
510 was performed as described in Liu *et al.*³⁸ with the modifications described in Dyson *et al.*²⁵.

511 **Selection, expression, and purification of IgGs**

512 Based on ranking and cross-reactivity in IgG binding in ENC assay, IgG expression yield, HPLC-
513 SEC profile, AS-SINS shift, and sequence diversity six antibodies (2551_01_A12, 2551_01_B11,
514 2554_01_D11, 2555_01_A01, 2555_01_A04, and 2558_02_G09) were selected for further
515 characterization. The IgGs were expressed and purified as previously described⁶.

516

517 **Surface plasmon resonance**

518 The binding affinity of the corresponding Fab versions of the top six affinity matured antibodies
519 as well as the parental clone to α -cobratoxin and Dp7 was determined using Surface Plasmon
520 Resonance (SPR) (BIAcore T100, GE Healthcare). Antigen immobilization and affinity
521 measurements were performed as previously described⁸. Based on affinity measurements the top
522 two clones for further characterization were selected to be 2551_01_A12 and 2554_01_D11.

523 Epitope binning experiments were performed using a sandwich setup, whereby one antibody was
524 immobilized on a CM5 sensor chip using amine coupling, prior to flowing α -cobratoxin with a
525 competing antibody. The 2554_01_D11 Fab (10 μ g/mL, 10mM sodium acetate pH5.0) was
526 immobilized to a level of 450RU, and 20nM α -cobratoxin (10mM, HEPES, 150 mM NaCl, 50 mM
527 MES, 0.05% P20, pH7.4) was incubated with 200nM of either test 2552_02_B02 Fab or control
528 Fab. Dual binding was then measured by injecting the α -cobratoxin and Fab solution over the
529 immobilized 2554_01_D11 flow cell for 120s. A blank flow cell was used as a reference, and was
530 subtracted from the test flow cell for analysis.

531 **Determining cross-reactivity using native mass spectrometry**

532 *Sample preparation*

533 Venoms and antibody samples were fractionated and exchanged into 200 mM ammonium acetate
534 by size exclusion chromatography (SEC) as previously described^{39,40}. These experiments were
535 performed on a Superdex Increase 200 10/300 GL column (Cytiva, Massachusetts, United States)
536 pre-equilibrated with 200 mM ammonium acetate. Samples were collected and stored at 4 °C until
537 used. Prior to analysis, aliquots of the venom and IgG 2554_01_D11 SEC fractions were mixed in
538 a 1:1 ratio (v/v). The final concentration of the antibody was approximately 3 μ M after mixing.

539 The concentration of toxins in the SEC fractions were not adjusted prior to mixing with the
540 antibody.

541 *Native mass spectrometry*

542 All mass spectrometry (MS) experiments were performed on a SELECT SERIES cyclic IMS mass
543 spectrometer (Waters, Manchester, U.K.) which was fitted with a 32,000 m/z quadrupole, as well
544 as an electron capture dissociation (ECD) cell (MSvision, Almere, Netherlands), the latter of which
545 was situated in the transfer region of this mass spectrometer. Approximately 4 μ L of sample were
546 nano-sprayed from borosilicate capillaries (prepared in-house) fitted with a platinum wire. Spectra
547 were acquired in a positive mode, with the m/z range set to 50-8,000. Acquisitions were performed
548 for five minutes at a rate of 1 scan per second. The operating parameters for the MS experiments
549 were as follows, unless otherwise stated: capillary voltage, 1.2 - 1.5 kV; sampling cone, 20 V;
550 source offset, 30 V; source temperature, 28 °C; trap collision energy, 5 V; transfer collision energy,
551 5 V; Ion guide RF, 700 V. This instrument was calibrated with a 50:50 acetonitrile:water solution
552 containing 20 μ M cesium iodide (99.999%, analytical standard for HR-MS, Fluka, Buchs,
553 Switzerland) each day prior to measurements.

554 *Top-down proteomics of toxins bound by 2554_01_D11*

555 The toxin:antibody complexes were purified using SEC, using the methods described above.
556 Toxins were ejected from the protein complex during the MS experiments by setting the cone
557 voltage to 160 V. The 5⁺ ions (most abundant charge state) of the ejected toxins were selected by
558 tandem MS (MS/MS) and subjected to fragmentation by applying a trap voltage between 80 and
559 100 V as well as a transfer voltage between 20 and 50 V. Peptide sequence assignment was

560 performed for 1⁺ fragmentation ions using the BioLynx package, which is a part of the MassLynx
561 v4.1 software.

562 **Sequence alignment**

563 Sequence alignment was performed in Clustal Omega⁴¹ and visualised in Jalview⁴² using α -
564 cobra toxin (P01391) from *N. kaouthia*, α -elapitoxin (P01396) from *D. polylepis*, α -bungarotoxin
565 (P60615) from *B. multicinctus*, long neurotoxin 2 (A8N285) from *O. hannah*, and long neurotoxin
566 (P0DQQ2) and long neurotoxin 2 (P01388) from *N. melanoleuca*. Structures for each toxin were
567 retrieved prioritising high-resolution X-ray resolved structures and included the following: P01391
568 = 1CTX (2.8 \AA , X-ray), P01388 = AF-P01388-F1 (AlphaFold2 predicted), P01396 = AF-P01396-
569 F1 (AlphaFold2 predicted), P60615 = 1HC9 (1.8 \AA , X-ray), A8N285 = AF-A8N285-F1
570 (AlphaFold2 predicted), and P0DQQ2 = AF-P0DQQ2-F1 (AlphaFold2 predicted). Structural
571 alignment and root-mean-square deviation (RMSD) analysis were performed in ChimeraX⁴³.
572 Epitopes of P01388 and P01396 were identified using the STAB Profiles tool³⁰
573 (https://venom.shinyapps.io/stab_profiles/).

574 ***In vitro* neutralization using electrophysiology (QPatch)**

575 To determine the ability and potency with which the affinity matured clones 2551_01_A12 and
576 2554_01_D11, as well as the parental antibody 368_01_C05, were able to neutralize the effects of
577 α -cobra toxin, whole-cell patch-clamp experiments were conducted using Rhabdomyosarcoma
578 cells (ACTT) as previously described⁸. In brief, the nAChR-mediated current elicited by
579 acetylcholine was determined in the presence of 4 nM α -cobra toxin or 4 nM α -cobra toxin
580 preincubated with different concentrations of the three IgGs on a QPatch II automated
581 electrophysiology platform (Sophion Bioscience). As a control a dendrotoxin-specific IgG was
582 included. The inhibitory effect of α -cobra toxin was normalized to the full acetylcholine response

583 and a non-cumulative concentration-response plot was plotted. A Hill fit was used to obtain IC₅₀
584 values for each of the three IgGs.

585 ***In vitro* cross-neutralization using electrophysiology (Qube 384)**

586 To determine the broader cross-neutralizing potential of the top two affinity matured antibodies
587 and the parent antibody, automated patch-clamp experiments using the Qube 384
588 electrophysiology platform (Sophion Bioscience) were conducted. The three IgGs (32.5 nM) were
589 tested against α -cobratoxin (1.47 nM), α -bungarotoxin (6.5 nM), Dp7 (0.81 nM), Nm8 (14 nM),
590 Nm3 (10.3 nM). A dendrotoxin-specific IgG was included as a control.

591 **Animals**

592 Animal experiments were conducted in CD-1 mice of both sexes weighing 18-20 g. Mice were
593 supplied by Instituto Clodomiro Picado and experiments were conducted following protocols
594 approved by the Institutional Committee for the Use and Care of Animals (CICUA), University of
595 Costa Rica (approval number CICUA 82-08). Mice were provided food and water *ad libitum* and
596 housed in plastic cages in groups of 4.

597 ***In vivo* preincubation experiments**

598 The *in vivo* cross-neutralizing potential of 2554_01_D11 against whole venoms of *N. kaouthia*, *D.*
599 *polylepis*, and *O. hannah* was assessed by i.v. injection of IgG preincubated with venom using
600 groups of four mice per treatment. Mixtures of a constant amount of venom and various amounts
601 of antibody were prepared and incubated for 30 min at 37 °C. Then, aliquots of the mixtures,
602 containing 2 LD₅₀s of venoms (for *N. kaouthia* 9.12 μ g, for *D. polylepis* 25.8 μ g, and for *O. hannah*
603 40 μ g) were injected in the caudal vein of mice using an injection volume of 150-200 μ L. Control
604 mice were injected with either venom alone, venom preincubated with an isotype control IgG or,

605 in the cases of *N. kaouthia* and *D. polylepis* venoms, they were preincubated with commercial
606 horse-derived antivenoms. For *N. kaouthia* Snake Venom Antiserum from VINS Bioproducts
607 Limited (Batch number: 01AS13100) was used at a ratio of 0.2 mg venom per mL antivenom. For
608 *D. polylepis* Premium Serum and Vaccines antivenom (Batch number: 062003) was used at a ratio
609 of 0.12 mg venom per mL antivenom.

610 The IgG was injected using 1:1 and 1:2 α -neurotoxin:IgG molar ratio for *N. kaouthia* and *O.*
611 *hannah* and 1:3 α -neurotoxin:IgG molar ratio for *D. polylepis*. For calculating molar ratios, based
612 on toxicovenomic studies, it was estimated that 55% of *N. kaouthia* venom¹⁷, 13.2% of *D. polylepis*
613 venom¹⁸, and 40% of *O. hannah* consisted of α -neurotoxins⁴⁴. Following injection, animals were
614 observed for signs of neurotoxicity, and survival was monitored for 48 hours. Results were
615 presented in Kaplan-Meier plots.

616 ***In vivo* rescue-type experiments**

617 In order to assess whether the antibody was capable of neutralizing the venom of *N. kaouthia* in
618 an experimental setting that more closely resembles the actual circumstances of envenoming, a
619 rescue-type experiment was designed. For this, the s.c. route was used for injection of venom,
620 while the antibody was administered i.v. First, the s.c. LD₅₀ of *N. kaouthia* venom was estimated
621 by injecting various doses of venom diluted in 100 μ L of PBS into groups of four mice. Animals
622 were observed during 24 hr, deaths were recorded and the LD₅₀ was estimated by probits⁴⁵. For
623 neutralization experiments, groups of four mice first received a challenge dose of a challenge dose
624 of 20.6 mg of venom by the s.c. route, corresponding to 2 LD₅₀s. Then, mice receiving antibody
625 2554_01_D11 immediately following venom administration, 535 μ g of antibody was administered
626 i.v. in the caudal vein (in a volume of 100 μ L) corresponding to a 1:2.5 toxin to antibody molar
627 ratio. For mice receiving antibody 10 min after envenoming, 412 μ g of the 2554_01_D11 antibody

628 were administered i.v. in the caudal vein (in a volume of 100 μ L), corresponding to a toxin to
629 antibody molar ratio of 1:2. Mice were observed for the onset of neurotoxic manifestations and
630 times of death were recorded and presented in Kaplan-Meier plots.

631 **References**

632 1. Gutiérrez, J. M. *et al.* Snakebite envenoming. *Nat. Rev. Dis. Primer* **3**, 1–21 (2017).

633 2. Pucca, M. B. *et al.* History of Envenoming Therapy and Current Perspectives. *Front.*
634 *Immunol.* **10**, 1598 (2019).

635 3. Hamza, M. *et al.* Clinical management of snakebite envenoming: Future perspectives. *Toxicon*
636 *X* **11**, 100079 (2021).

637 4. Laustsen, A. H. Antivenom in the Age of Recombinant DNA Technology. in *Handbook of*
638 *Venoms and Toxins of Reptiles* (CRC Press, 2021).

639 5. Richard, G. *et al.* In Vivo Neutralization of α -Cobratoxin with High-Affinity Llama Single-
640 Domain Antibodies (VHHs) and a VHH-Fc Antibody. *PLOS ONE* **8**, e69495 (2013).

641 6. Laustsen, A. H. *et al.* In vivo neutralization of dendrotoxin-mediated neurotoxicity of black
642 mamba venom by oligoclonal human IgG antibodies. *Nat. Commun.* **9**, 3928 (2018).

643 7. Ahmadi, S. *et al.* An in vitro methodology for discovering broadly-neutralizing monoclonal
644 antibodies. *Sci. Rep.* **10**, 10765 (2020).

645 8. Ledsgaard, L. *et al.* In vitro discovery of a human monoclonal antibody that neutralizes
646 lethality of cobra snake venom. *mAbs* **14**, 2085536 (2022).

647 9. Casewell, N. R., Jackson, T. N. W., Laustsen, A. H. & Sunagar, K. Causes and Consequences
648 of Snake Venom Variation. *Trends Pharmacol. Sci.* **41**, 570–581 (2020).

649 10. Kini, R. M., Sidhu, S. S. & Laustsen, A. H. Biosynthetic Oligoclonal Antivenom (BOA)
650 for Snakebite and Next-Generation Treatments for Snakebite Victims. *Toxins* **10**, 534 (2018).

651 11. Jenkins, T. P. & Laustsen, A. H. Cost of Manufacturing for Recombinant Snakebite
652 Antivenoms. *Front. Bioeng. Biotechnol.* **8**, (2020).

653 12. Ledsgaard, L. *et al.* Antibody Cross-Reactivity in Antivenom Research. *Toxins* **10**, E393
654 (2018).

655 13. Laustsen, A. H., Johansen, K. H., Engmark, M. & Andersen, M. R. Recombinant
656 snakebite antivenoms: A cost-competitive solution to a neglected tropical disease? *PLoS Negl.*
657 *Trop. Dis.* **11**, e0005361 (2017).

658 14. Laustsen, A. H., Greiff, V., Karatt-Vellatt, A., Muyldermans, S. & Jenkins, T. P. Animal
659 Immunization, in Vitro Display Technologies, and Machine Learning for Antibody Discovery.
660 *Trends Biotechnol.* (2021) doi:10.1016/j.tibtech.2021.03.003.

661 15. Roncolato, E. C. *et al.* Phage display as a novel promising antivenom therapy: A review.
662 *Toxicon* **93**, 79–84 (2015).

663 16. Tan, K. Y., Tan, C. H., Fung, S. Y. & Tan, N. H. Venomics, lethality and neutralization
664 of *Naja kaouthia* (monocled cobra) venoms from three different geographical regions of
665 Southeast Asia. *J. Proteomics* **120**, 105–125 (2015).

666 17. Laustsen, A. H. *et al.* Snake venomics of monocled cobra (*Naja kaouthia*) and
667 investigation of human IgG response against venom toxins. *Toxicon Off. J. Int. Soc.*
668 *Toxinology* **99**, 23–35 (2015).

669 18. Laustsen, A. H., Lomonte, B., Lohse, B., Fernandez, J. & Gutierrez, J. M. Unveiling the
670 nature of black mamba (*Dendroaspis polylepis*) venom through venomics and antivenom
671 immunoprofiling: Identification of key toxin targets for antivenom development. *J.*
672 *Proteomics* **119**, 126–142 (2015).

673 19. Ainsworth, S. *et al.* The medical threat of mamba envenoming in sub-Saharan Africa
674 revealed by genus-wide analysis of venom composition, toxicity and antivenomics profiling of
675 available antivenoms. *J. Proteomics* **172**, 173–189 (2018).

676 20. Rodríguez-Rodríguez, E. R. *et al.* Broadening the neutralizing capacity of a family of
677 antibody fragments against different toxins from Mexican scorpions. *Toxicon* **119**, 52–63
678 (2016).

679 21. Marks, J. D. *et al.* By-Passing Immunization: Building High Affinity Human Antibodies
680 by Chain Shuffling. *Bio/Technology* **10**, 779–783 (1992).

681 22. Alkondon, M. & Albuquerque, E. X. α -Cobratoxin blocks the nicotinic acetylcholine
682 receptor in rat hippocampal neurons. *Eur. J. Pharmacol.* **191**, 505–506 (1990).

683 23. Wang, C.-I. A. *et al.* Isolation and structural and pharmacological characterization of α -
684 elapitoxin-Dpp2d, an amidated three finger toxin from black mamba venom. *Biochemistry* **53**,
685 3758–3766 (2014).

686 24. Lauridsen, L. P., Laustsen, A. H., Lomonte, B. & Gutiérrez, J. M. Exploring the venom
687 of the forest cobra snake: Toxicovenomics and antivenom profiling of *Naja melanoleuca*. *J.*
688 *Proteomics* **150**, 98–108 (2017).

689 25. Dyson, M. R. *et al.* Beyond affinity: selection of antibody variants with optimal
690 biophysical properties and reduced immunogenicity from mammalian display libraries. *mAbs*
691 **12**, 1829335 (2020).

692 26. Sintiprungrat, K. *et al.* A comparative study of venomics of *Naja naja* from India and Sri
693 Lanka, clinical manifestations and antivenomics of an Indian polyspecific antivenom. *J.*
694 *Proteomics* **132**, 131–143 (2016).

695 27. Lermyte, F., Tsybin, Y. O., O'Connor, P. B. & Loo, J. A. Top or Middle? Up or Down?
696 Toward a Standard Lexicon for Protein Top-Down and Allied Mass Spectrometry
697 Approaches. *J. Am. Soc. Mass Spectrom.* **30**, 1149–1157 (2019).

698 28. Mitchell Wells, J. & McLuckey, S. A. Collision-Induced Dissociation (CID) of Peptides
699 and Proteins. in *Methods in Enzymology* vol. 402 148–185 (Academic Press, 2005).

700 29. Lingdong Quan, M. L. CID,ETD and HCD Fragmentation to Study Protein Post-
701 Translational Modifications. *Mod. Chem. Appl.* **01**, (2013).

702 30. Krause, K. E. *et al.* An interactive database for the investigation of high-density peptide
703 microarray guided interaction patterns and antivenom cross-reactivity. *PLoS Negl. Trop. Dis.*
704 **14**, e0008366 (2020).

705 31. Bourne, Y., Talley, T. T., Hansen, S. B., Taylor, P. & Marchot, P. Crystal structure of a
706 Cbtx–AChBP complex reveals essential interactions between snake α -neurotoxins and
707 nicotinic receptors. *EMBO J.* **24**, 1512–1522 (2005).

708 32. Tan, C. H., Tan, K. Y., Fung, S. Y. & Tan, N. H. Venom-gland transcriptome and venom
709 proteome of the Malaysian king cobra (*Ophiophagus hannah*). *BMC Genomics* **16**, 687
710 (2015).

711 33. Fruchart-Gaillard, C. *et al.* Experimentally based model of a complex between a snake
712 toxin and the α 7 nicotinic receptor. *Proc. Natl. Acad. Sci.* **99**, 3216–3221 (2002).

713 34. Rusmili, M. R. A., Yee, T. T., Mustafa, M. R., Hodgson, W. C. & Othman, I. Proteomic
714 characterization and comparison of Malaysian *Bungarus candidus* and *Bungarus fasciatus*
715 venoms. *J. Proteomics* **110**, 129–144 (2014).

716 35. Malih, I. *et al.* Proteomic analysis of Moroccan cobra *Naja haje legionis* venom using
717 tandem mass spectrometry. *J. Proteomics* **96**, 240–252 (2014).

718 36. Knudsen, C. *et al.* Novel Snakebite Therapeutics Must Be Tested in Appropriate Rescue
719 Models to Robustly Assess Their Preclinical Efficacy. *Toxins* **12**, 528 (2020).

720 37. Schofield, D. J. *et al.* Application of phage display to high throughput antibody
721 generation and characterization. *Genome Biol.* **8**, R254 (2007).

722 38. Liu, Y. *et al.* High-throughput screening for developability during early-stage antibody
723 discovery using self-interaction nanoparticle spectroscopy. *mAbs* **6**, 483–492 (2014).

724 39. Wang, C. R., Bubner, E. R., Jovcevski, B., Mittal, P. & Pukala, T. L. Interrogating the
725 higher order structures of snake venom proteins using an integrated mass spectrometric
726 approach. *J. Proteomics* **216**, 103680 (2020).

727 40. Harrison, J. A. & Aquilina, J. A. Insights into the subunit arrangement and diversity of
728 paradoxin and taipoxin. *Toxicon Off. J. Int. Soc. Toxinology* **112**, 45–50 (2016).

729 41. Madeira, F. *et al.* The EMBL-EBI search and sequence analysis tools APIs in 2019.
730 *Nucleic Acids Res.* **47**, W636–W641 (2019).

731 42. Waterhouse, A. M., Procter, J. B., Martin, D. M. A., Clamp, M. & Barton, G. J. Jalview
732 Version 2—a multiple sequence alignment editor and analysis workbench. *Bioinformatics* **25**,
733 1189–1191 (2009).

734 43. Pettersen, E. F. *et al.* UCSF ChimeraX: Structure visualization for researchers, educators,
735 and developers. *Protein Sci. Publ. Protein Soc.* **30**, 70–82 (2021).

736 44. Petras, D., Heiss, P., Süssmuth, R. D. & Calvete, J. J. Venom Proteomics of Indonesian
737 King Cobra, *Ophiophagus hannah*: Integrating Top-Down and Bottom-Up Approaches. *J.*
738 *Proteome Res.* **14**, 2539–2556 (2015).

739 45. Finney, D. *Probits analysis*. (Cambridge University Press, 1971).

740

741

742

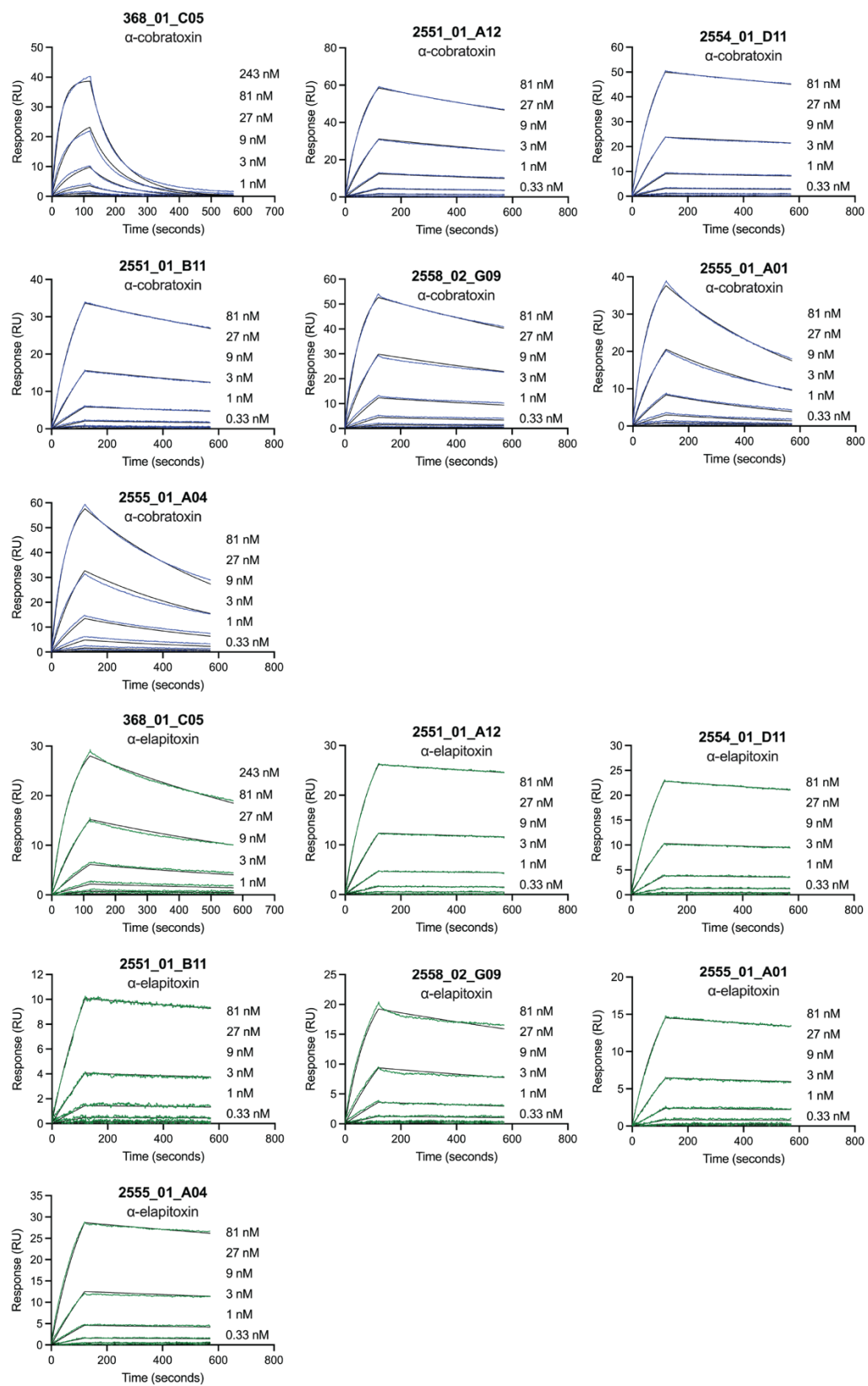
743 **Supplementary material**

744 **Table S1. Expression and developability data for 61 IgGs and parental IgG.** The expression
745 yield is provided for cultures in 96-well format. AC-SINS shift reflects IgG self-association
746 propensity and SEC analysis provides information on elution volume as well as percentage of IgG
747 monomer and dimers detected.

Antibody ID	Production	AC-SINS	SEC analysis		
	Yield (mg/L)	Shift (nm)	Elution (mL)	Monomer (%)	Dimer (%)
2551_01_A12	7,7	3	1,48	100,0	0,0
2554_01_D11	14,0	1	1,48	94,8	5,2
2552_02_B07	10,7	1	1,47	97,1	2,9
2558_02_G09	21,7	1	1,48	95,6	4,4
2551_01_A11	10,6	2	1,50	95,2	4,8
2554_01_E01	15,5	2	1,49	96,6	3,4
2551_01_B11	11,1	1	1,50	96,2	3,8
2554_02_F10	23,6	1	1,48	96,5	3,5
2551_01_A02	11,3	1	1,46	97,0	3,0
2552_01_G02	11,7	2	1,49	96,6	3,4
2554_01_E10	12,2	1	1,47	95,2	4,8
2554_02_F11	13,9	1	1,48	94,4	5,6
2555_01_A04	8,7	1	1,47	100,0	0,0
2555_01_A01	16,0	1	1,47	96,7	3,3
2554_02_G09	14,8	4	1,48	97,0	3,0
2558_01_E06	15,2	1	1,47	96,3	3,7
2554_01_E03	14,5	1	1,48	96,6	3,4
2554_01_C11	14,4	1	1,47	97,2	2,8
2554_01_D10	13,2	1	1,47	96,8	3,2
2554_01_E05	9,8	2	1,46	96,9	3,1
2555_02_D09	14,8	2	1,46	97,0	3,0
2555_02_D02	7,3	1	1,49	100,0	0,0
2555_01_B09	16,5	1	1,47	96,0	4,0
2554_01_D05	13,9	2	1,47	97,1	2,9
2554_01_C07	14,0	2	1,47	96,6	3,4

2558_01_E08	13,1	1	1,47	96,7	3,3
2554_02_G10	13,6	1	1,47	96,9	3,1
2558_02_F12	12,9	1	1,47	96,6	3,4
2555_02_D05	11,4	2	1,47	100,0	0,0
2551_02_E01	11,3	2	1,52	95,2	4,8
2558_02_H05	10,0	2	1,49	96,6	3,4
2558_02_G01	8,0	3	1,48	100,0	0,0
2558_02_G10	17,2	2	1,48	96,4	3,6
2551_01_B01	12,2	1	1,43	96,5	3,5
2554_02_H01	9,1	1	1,48	96,5	3,5
2554_02_G12	13,9	2	1,56	100,0	0,0
2554_01_D01	9,9	2	1,51	97,1	2,9
2551_01_A01	2,7	7	1,49	100,0	0,0
2554_02_G07	15,9	1	1,48	96,6	3,4
2554_02_F12	11,4	1	1,47	95,3	4,7
2555_01_B01	19,7	1	1,48	95,4	4,6
2558_01_E04	12,1	1	1,51	95,6	4,4
2558_02_H06	9,3	1	1,47	100,0	0,0
2558_01_E03	20,1	1	1,47	96,1	3,9
2558_01_D11	15,4	1	1,47	97,2	2,8
2558_02_G07	17,9	0	1,46	96,4	3,6
2555_01_B04	17,3	1	1,48	97,4	2,6
2558_02_G02	20,1	-1	1,48	96,2	3,8
2558_01_E02	10,7	2	1,48	100,0	0,0
2555_02_D06	21,4	0	1,46	96,9	3,1
2554_01_D09	7,3	2	1,46	100,0	0,0
2555_02_D07	17,2	0	1,48	96,2	3,8
2558_01_D12	15,6	1	1,47	95,9	4,1

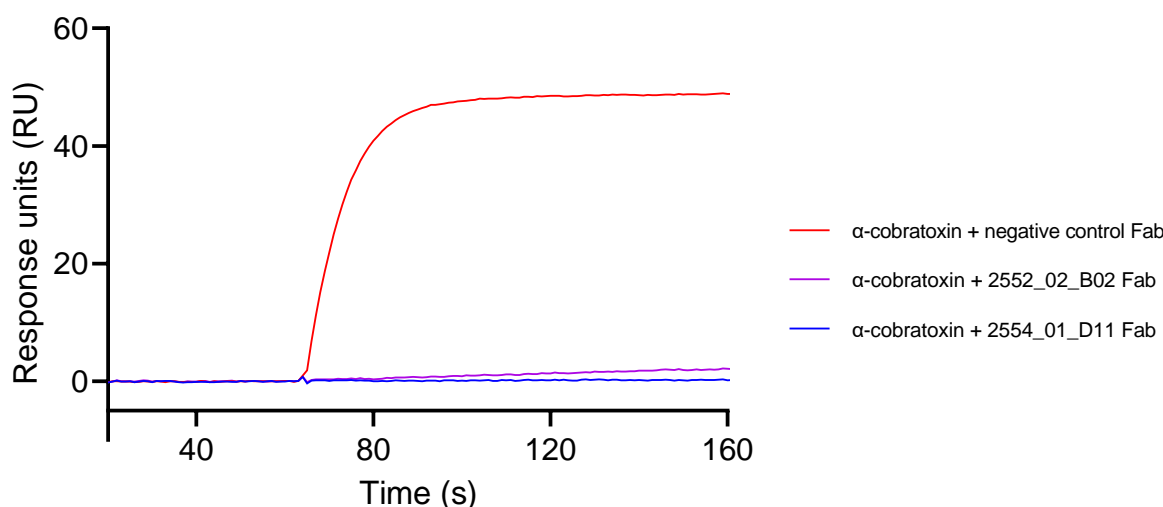
2558_02_G03	14,4	1	1,49	91,1	8,9
2558_01_E10	16,7	0	1,48	96,6	3,4
2558_02_G04	17,6	0	1,46	97,3	2,7
2554_01_D04	3,8	3	1,47	100,0	0,0
2554_02_F04	18,9	-	1,49	95,5	4,5
2555_02_C08	16,2	-	1,55	97,2	2,8
2558_02_G05	15,1	-	1,47	97,0	3,0
2555_01_A08	12,3	-	1,48	96,1	3,9
2558_02_F10	6,9	-	1,47	100,0	0,0
368_01_C05	14,7	0	1,45	97,5	2,5



750 **Fig. S1. Affinity measurements using surface plasmon resonance.** Sensograms illustrating
751 affinity measurements of the top six affinity matured antibodies as well as the parent on α -
752 cobra toxin and α -elapitoxin immobilized on a CM5 sensor.

753

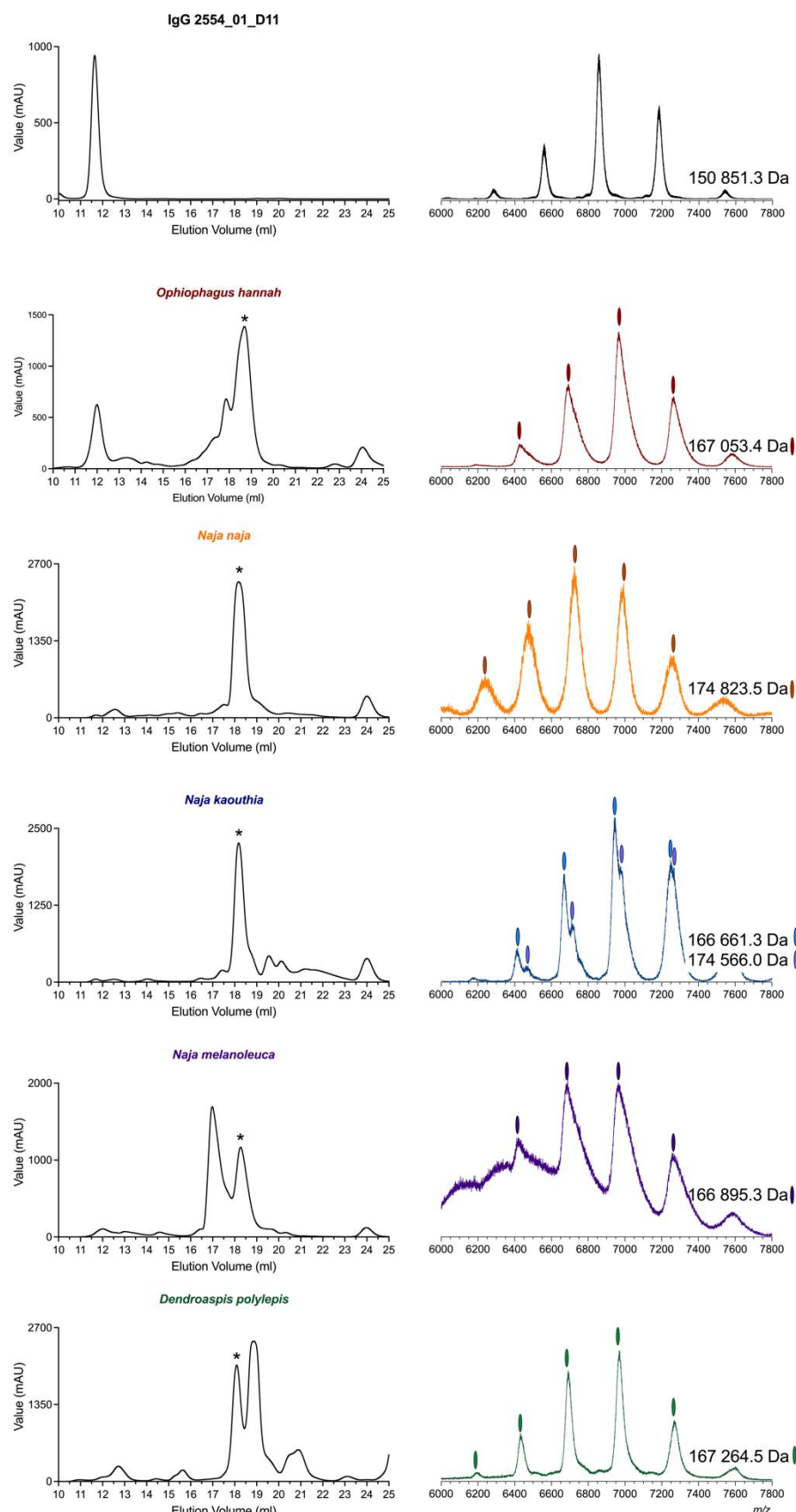
754



755
756 **Fig. S2. Epitope binning of 2554_01_D11 and 2552_02_B02 anti- α -cobra toxin Fabs by SPR.**

757 Sensorgrams of α -cobra toxin interacting with immobilized 2554_01_D11 Fab in the presence of
758 2552_02_B02 Fab. 200 nM of Fab was pre-incubated for 30 min with 20 nM α -cobra toxin
759 before being flowed over immobilized 2554_01_D11 for 120s. A non α -cobra toxin specific Fab
760 and the 2554_01_D11 Fab were included as negative and positive controls, respectively.

761



763 **Fig S3. Size exclusion chromatograms of the snake whole venoms and native mass spectra of**
764 **toxin:antibody complexes.** Size exclusion chromatograms of IgG 2554_01_D11 and five featured
765 venoms accompanied by native mass spectra of IgG 2554_01_D11 – toxin fraction with asterix
766 from each SEC run.

767